European Journal of Pharmaceutics and Biopharmaceutics 74 (2010) 239–247

Contents lists available at ScienceDirect

European Journal of Pharmaceutics and Biopharmaceutics

journal homepage: www.elsevier.com/locate/ejpb

Research paper

Characterization of the copolymer poly(ethyleneglycol-g-vinylalcohol) as a potential carrier in the formulation of solid dispersions

Sandra Guns [a], Pieterjan Kayaert [a], Johan A. Martens [b], Jan Van Humbeeck [c], Vincent Mathot [d,e], Thijs Pijpers [d,e], Evgeny Zhuravlev [f], Christoph Schick [f], Guy Van den Mooter [a,*]

[a] Laboratory for Pharmacotechnology and Biopharmacy, Catholic University of Leuven, Leuven, Belgium
[b] Centre for Surface Chemistry and Catalysis, Catholic University of Leuven, Heverlee, Belgium
[c] Department of Metallurgy and Materials Engineering, Catholic University of Leuven, Heverlee, Belgium
[d] SciTe B.V., Geleen, The Netherlands
[e] Department of Chemistry, Catholic University of Leuven, Heverlee, Belgium
[f] Department of Polymer Physics, University of Rostock, Rostock, Germany

ARTICLE INFO

Article history:
Received 7 August 2009
Accepted in revised form 20 September 2009
Available online 24 September 2009

Keywords:
Poly(ethyleneglycol-g-vinylalcohol) (EG/VA, Kollicoat® IR)
Differential Scanning Calorimetry (DSC)
High Performance Differential Scanning Calorimetry (HPer DSC)
X-ray powder diffraction (XRPD)
Chip calorimetry
Solid dispersion

ABSTRACT

In order to fully exploit the graft copolymer poly(ethyleneglycol-g-vinylalcohol) (EG/VA) in the formulation of solid dispersions, a characterization of its phase behavior before, during and after spray-drying and hot-melt extrusion is performed. Solid state characterization was performed using MDSC and XRPD. The effect of heating/cooling rate on the degree of crystallinity was studied using HPer DSC and ultra-fast chip calorimetry. EG/VA consists of two semi-crystalline fractions, one corresponding to the polyethyleneglycol (PEG) fraction (T_g = −57 °C, T_m = 15 °C) and one corresponding to the polyvinylalcohol (PVA) fraction (T_g = 45 °C, T_m = 212 °C). XRPD analysis confirmed its semi-crystallinity, and EG/VA showed Bragg reflections comparable to those of PVA. Spray-drying at a temperature lower than 170 °C resulted in amorphization of the PVA fraction, while after hot-melt extrusion at different temperatures, the crystallinity of this fraction increases. In both cases, the PEG fraction is not influenced. Plasticization of the amorphous domains of the PEG or PVA fraction of the copolymer was dependent on the type and concentration of plasticizer, suggesting that also other small organic molecules like drugs may not homogeneously mix with both amorphous domains. A controlled cooling rate of 3000 °C/s was necessary to make the copolymer completely amorphous.

1. Introduction

Permeability and solubility are two key determinants of the oral bio-availability of drug components. Since combinatorial chemistry and high-throughput screening of potential therapeutic agents are systematically used in the pharmaceutical industry, the molecular complexity and hydrophobicity of pharmacologically active compounds have significantly increased during the past two decades. Compounds with molecular weights over 500 Da are no longer an exception. The majority of these compounds have a very low water solubility leading to oral bio-availability which will be too low to be therapeutically effective [1].

A well-established strategy to enhance oral bio-availability is the formulation of poorly soluble drugs in solid dispersions. According to Chiou and Riegelman, the term "solid dispersion" refers to the dispersion of one or more active ingredients in an inert carrier or matrix at solid state prepared by the melting (fusion), solvent or melting-solvent method. These methods can result in different classes of solid dispersions such as simple eutectic mixtures, solid solutions, glass solutions and glass suspensions, amorphous precipitations of a drug in a crystalline carrier, compound or complex formations between the drug and the carrier and any combinations among previously mentioned groups [2,3].

A first generation of carriers used for solid dispersion formulations were highly water soluble, low molecular weight crystalline carriers, such as urea and sugars. However, currently, fully synthetic polymers including polyvinylpyrrolidone (PVP), polyethyleneglycols (PEG), polymethacrylates and natural product-based polymers as cellulose derivates (HPMC, HPC, CMEC, HPMCP) are used to formulate solid dispersions. These systems are able to produce amorphous forms of the drug and carriers, to reduce the drug particle size to a molecular level (glass solutions), to solubilize or co-dissolve the drug by the water soluble carrier and to provide better wettability and dispersibility of the drug by the carrier material. The carrier dissolution dictates the drug release from

* Corresponding author. Laboratory for Pharmacotechnology and Biopharmacy, Catholic University of Leuven, K.U. Leuven, Gasthuisberg O&N2, Herestraat 49, Box 921, 3000 Leuven, Belgium. Tel.: +32 16 330 304; fax: +32 16 330 305.
E-mail address: Guy.VandenMooter@pharm.kuleuven.be (G. Van den Mooter).

0939-6411/$ - see front matter © 2009 Elsevier B.V. All rights reserved.
doi:10.1016/j.ejpb.2009.09.009

glass solutions, which can even be improved if the carrier has surface active properties [3]. The number of useful polymers is relatively limited today, so the search for new materials is important for the pharmaceutical industry.

Recently, we found a graft copolymer of ethyleneglycol and vinylalcohol to be potentially useful in the formulation of solid dispersions. This copolymer was originally developed by BASF as a coating material for instant release tablets and is marketed under the trade mark Kollicoat® IR. The polymer consists of 75% polyvinyl alcohol units grafted on 25% polyethylene glycol units. Its solubility is 40% (w/w) in aqueous systems and 25% (w/w) in a 1:1 ethanol–water mixture; the solubility in non-polar solvents is low [4]. This hydrophilic polymer is slightly surface active and semi-crystalline; according to the manufacturer, the polyethylene glycol moiety can act as an internal plasticizer [5].

From a theoretical point of view, it is an interesting polymer to be used as a carrier for the formulation of solid dispersions. As it is hydrophilic and non-ionic, its solubility does not change along with the gastrointestinal tract. It is slightly surface active, which can be useful to maintain supersaturation of poorly soluble drugs in the gastrointestinal tract.

Initial studies showed that solid dispersions of poly(ethyleneglycol-g-vinylalcohol) (EG/VA) and itraconazole prepared by hot-melt extrusion significantly increased drug dissolution and maintained supersaturation for a couple of hours in simulated gastric fluid [6]. Recent studies of our group indicated the potential of this copolymer to be processed by spray-drying [7]. These results are promising, but in order to fully explore the possibilities of this polymer in its application as a carrier for solid dispersions, it is crucial to have a good understanding of the phase behavior of this semi-crystalline material before, during and after spray-drying and hot-melt extrusion. It is only with this information that the effect of small organic drug molecules and production process parameters on the copolymer's phase behavior can be evaluated, and its performances as a carrier in solid dispersions were fully appreciated.

The purpose of the present paper is to characterize EG/VA with respect to the co-existence of crystalline and amorphous domains before, during and after typical solid dispersion manufacturing processes like spray-drying and hot-melt extrusion. Next to well-established solid state characterization techniques such as MDSC and XRPD, we also describe the use of HPer DSC and ultra-fast chip calorimetry as a techniques to study the influence of heating/cooling rate on (cold- and re)crystallization, reorganization and melting.

2. Materials and methods

2.1. Materials

The grafted copolymer of polyethylene glycol and polyvinyl alcohol (Mw = ca. 45,000 Da) was obtained from BASF (Ludwigshafen, Germany). Polyvinylalcohol (PVA, Mw = ca. 9500 Da) was obtained from Sigma–Aldrich (Schnelldorf, Germany), and polyethyleneglycol (PEG, Mw = ca. 2000 Da) was obtained from Fagron NV (Waregem, Belgium). Propyleneglycol was obtained from Alpha Pharma (PG, Nazareth, Belgium), PEG400 (Mw = ca. 400 Da) from Fagron NV (Waregem, Belgium), and diethyl phthalate was obtained from UCB (DEP, Brussels, Belgium).

2.2. Sample preparation

2.2.1. Spray-drying

The spray-drying process was performed using a Büchi mini spray dryer B-191 (Büchi, Flawil, Switzerland). The polymer was spray dried from a 5% (w/v%) solution in 100 ml solvent. During spray-drying, the solution was continuously stirred with a magnetic stirrer. The inlet temperature was varied from 80 °C to 170 °C, and the pump rate was chosen in relation to the solvent mixture and the inlet temperature (25% or 30%). The aspirator was always set at 100% and the air flow at 600 L/h.

Table 1
Overview of the different solutions and process parameters used during spray-drying.

Plasticizer	Solvent mixture	Inlet temperature (°C)	Pump rate (%)
None	H_2O	80	30
None	H_2O	110	30
None	H_2O	140	30
None	H_2O	170	30
None	H_2O	80	25
None	H_2O–EtOH (1:1)	80	25
None	H_2O–EtOH–CH_2Cl_2 (1:2:1)	80	25
None	H_20–EtOH (1:1)	90	25
DEP 10%	H_20–EtOH (1:1)	90	25
DEP 30%	H_20–EtOH (1:1)	90	25
PG 10%	H_2O	110	30
PG 30%	H_2O	110	30
PEG400 10%	H_2O	110	30
PEG400 30%	H_2O	110	30

All the solutions contained 5% poly(ethyleneglycol-g-vinylalcohol) and had a volume of 100 ml. The percentage plasticizer is expressed as a w/w percentage to the polymer. The aspirator was always set to 100%, and the air flow was always controlled at 600 L/h.

Three different solvents or mixtures thereof were used: water, ethanol or dichloromethane. The effect of three different plasticizers was tested, by adding them to the spray-dry solution (PEG400, propyleneglycol, diethyl phthalate) in a concentration of 10% or 30% (expressed as percentage of the polymer weight).

All spray-dried samples were further dried in a vacuum oven at 25 °C till constant mass and then stored in a dessicator (P_2O_5) and analyzed within 6 weeks.

An overview of the different solutions used for spray-drying is given in Table 1.

2.2.2. Hot-melt extrusion

A co-rotating mini twin screw extruder (DSM, Geleen, The Netherlands) was used in this study. The core of this extruder is formed by a mixing compartment consisting of two separable halves and double, conical mixing screws. It consists of two controlled heating zones, which were always kept at the same temperature, varying from 130 °C to 180 °C. The screw speed was set to 24, 44 or 108 rpm. A load of 5 g per run was fed manually into the hopper, and after feeding, the internal circulation time was 5 min. The core of the extruder was purged with nitrogen during extrusion. The extrudates were collected after air cooling at ambient temperature. All samples were stored in a freezer (−27 °C), protected from humidity and analyzed within 8 weeks.

An overview of the different experimental parameters that were varied during the extrusion tests can be found in Table 2.

Table 2
Overview of the extrusion temperature and screw speed used during hot-melt extrusion.

Extrusion temperature (°C)	Screw speed (rpm)
180	44
160	44
140	44
130	44
140	24
140	108

A load of 5 g was fed manually into the hopper, and the internal circulation time was 5 min. The extrudates were collected after air cooling at ambient temperature.

PVA was also extruded as reference material. A load of 5 g was fed manually into the hopper and the extrusion temperature was set to 160 °C, the rotation speed was 44 rpm, and the internal circulation time was 5 min.

2.3. Thermal analysis

2.3.1. Modulated temperature differential scanning calorimetry

MDSC measurements were carried out using a Q2000 modulated DSC (TA Instruments, Leatherhead, UK) equipped with a Refrigerated Cooling System (RCS90). Data were treated mathematically using Universal Analysis software (version 4.4A, TA Instruments, Leatherhead, UK). Glass transition temperatures were measured at half height in the reversing heat flow, and melting temperatures were measured at the peak maxima in the total heat flow. A flow rate of 50 ml/min of nitrogen was used as a purge gas through the DSC cell. TA Instruments standard aluminum pans (Brussels, Belgium) were used for all measurements. The sample masses varied from 4 to 10 mg (accurately weighed).

The DSC Tzero calibration was performed in two experiments, one without samples or pans (baseline) and the second was performed with large sapphire disks (without pans, weight approximately 100 mg). Octadecane, tin and indium standards were used to calibrate the DSC temperature scale, and enthalpic response was calibrated with indium. Heat capacity calibration was performed with a small sapphire disk in a pan. Validation of temperature and enthalpy showed that deviation of the experimental from the theoretical values was less then 0.1 °C for the temperature and less than 1% for the enthalpy measurements.

In order to find suitable measuring conditions for EG/VA, different set-ups were tested. Combinations of following modulation parameters were compared: an underlying heating rate of 1, 2.5 or 5 °C/min, an amplitude of ±0.10, ±0.20, ±0.40 or ±0.70 °C and a period of 10, 40, 70 or 100 s. Out of the 48 combinations that can be made with these conditions, an amplitude of ±0.40 °C, a period of 40 s and an underlying heating rate of 2.5 °C/min were selected for all measurements.

2.3.2. Thermogravimetric analysis

Thermogravimetric analysis was performed using a simultaneous DSC/TGA Q600 SDT (TA Instruments, Leatherhead, UK). The experiments were done using a heating rate of 5 °C/min under nitrogen atmosphere. The temperature was ramped from room temperature to 250 °C using a sample mass of ca. 7 mg. The loss in weight was evaluated using the Universal Analysis software (version 4.4A, TA Instruments, Leatherhead, UK).

2.3.3. High-speed calorimetry

All HPer DSC analysis were performed using a Perkin-Elmer Diamond DSC fitted with an Intracooler 2P-cooling unit (Perkin-Elmer, Massachusetts, USA). All measurements were taken under a helium gas purge at a flow rate of 30 ml/min. The calibration was performed as described earlier by Pijpers et al. [8]. A range of controlled cooling rates up to 500 °C/min were studied. Since the calibration was performed at relatively low scan rates (10 °C/min), the temperature data were corrected. A 15 μm thin aluminum foil was used to wrap the sample instead of using a pan as sample container. The aluminum foil has a much lower mass and provides a drastically improved way of heat transfer [8]. Data processing was performed using OriginPro 8 SRO software (version v8.0724(B724), OriginLab Corporation, Northampton, USA).

2.3.4. Ultra-fast chip calorimetry

An ultra-fast chip calorimeter developed by the group at Rostock University was used. The ultra-fast calorimeter is a thin-film chip calorimeter based on a thermal conductivity gauge XEN-39320 (Xensor Integration, Delfgauw, The Netherlands). The cell consists of a 1 μm thin-film silicon nitride membrane with a resistive film-heater and 6 film-thermopiles located at the center of the membrane [9,10]. The experiments were conducted using the system consisting of the sensor mounted inside an oven, immersed in liquid nitrogen. The instrument enables the measurements of the heat capacity of the investigated sample, according to the power compensation principle. Temperature correction was done using a small indium particle on top of the sample. More fully description of the system can be found elsewhere [11].

Scans with different controlled cooling rates (300°, 500°, 800°, 1000°, 3000° and 20,000 °C/s) were performed from 260 °C to −180 °C. Before cooling, the sample stays at 280 °C for only 1 ms to avoid degradation at such high temperature. Since the size of the sample is too small (ca. 30 μm sample size) to have a good signal at the low cooling rates, the reheating scan after cooling at the different rates was used for analysis. After each cooling step, the sample was reheated from −180 °C to 260 °C at 10,000 °C/s, and heat capacity was determined.

2.4. X-ray powder diffraction

X-ray powder diffraction (XRPD) was first performed at room temperature on the pure EG/VA, PVA, PEG and the spray-dried samples. An automated X'pert PRO diffractometer (PANalytical, Almelo, The Netherlands) was used in Bragg–Brentano geometry with a flat sample holder filled using the backloading technique to minimize preferred orientation. A copper tube with the generator set at 45 kV and 40 mA was used. Using a transmission–reflection spinner, it was possible to improve the counting statistics by spinning the sample using a rotation time of 4.0 s. In the incident beam path, a 0.04 rad soller slit, a 10 mm mask, a programmable divergence slit and a fixed anti-scatter slit of 4° were installed. In the diffracted beam path, a programmable anti-scatter slit, a 0.04 rad soller slit and a nickel filter (0.02 mm thick) were installed. Both the programmable divergence slit and the programmable anti-scatter slit were programmed to constantly irradiate 10 mm. The detector used for data collection was an X'Celerator RTMS detector, with an active length of 2.122°. The data were collected in continuous scan mode with a scan region of 4.0010° till 60.0005° and a step size of 0.0084°. The counting time was 40.005 s. X'pert data collector version 2.2c (PANalytical, Almelo, The Netherlands) was used for data collection, and X'pert data viewer version 1.2.a (PANalytical, Almelo, The Netherlands) was used for data visualization and treatment.

Secondly, XRPD was performed on pure EG/VA at temperatures different from room temperature. A reference diffractogram was recorded at 25 °C, before applying a temperature program. Subsequently, the sample was cooled down till −90 °C and then heated up till 230 °C; several diffractograms were collected at different temperatures. Afterwards, the material was cooled again till −90° and reheated till 25 °C. The X'per PRO diffractometer was therefore fitted with an Anton Paar non-ambient chamber model TTK 450 with liquid nitrogen cooling (Anton Paar, Graz, Austria). The incident- and diffracted beam path were configured similarly. Spinning was no longer possible, hence samples were front loaded. The same tube detector, data collector and viewer were used. Data were collected in a continuous scan mode with a scan region of 4.9830° till 38.0740° and a step size of 0.0501. The counting time was 40.005 s.

The last type of XRPD experiments were performed at room temperature on the extruded samples and on pure EG/VA, PVA and PEG in transmission geometry with transmission sample holders using Kapton foils to clamp the samples. The extrudates and the pure polymers (as a reference) were measured without crushing or any other sample preparation with a 2Theta scan. The transmission–reflection spinner was used with a sample rotation time of 4.0 s. In the incident

beam path, a focusing X-ray mirror, a 0.04 rad soller slit, a fixed divergence slit of 0.5° and a fixed anti-scatter slit of 1° were installed. In the diffracted beam path, a 0.04 rad soller silt and a programmable anti-scatter slit were installed. The last one was programmed to keep a fixed 0.5° opening. The same tube detector, data collector and viewer were used. The data were collected in continuous scan mode with a scan region of 3.9960° till 43.0001° and a step size of 0.0334°. The counting time was 59.690 s.

3. Results and discussion

3.1. Characterization of the unprocessed EG/VA

3.1.1. MDSC results

A broad endothermic signal between 20 and 100 °C made interpretation of the DSC data in this temperature range difficult (see total heat flow in Fig. 1A). This signal was allotted to the evaporation of water from the sample which was confirmed by TGA (a total weight loss of 4.6% when heated till 100 °C was recorded). Since drying at 25 °C in vacuum was not sufficient to remove the water, MDSC was used to investigate the thermal properties of pure EG/VA.

The MDSC heating curves of the pure polymer reported in Fig. 1A show several transitions. The evaporation of water is clearly visible in the non-reversing heat flow between 20 °C and 100 °C. Melting starts already early (around 170 °C), but the peak is situated at 212 °C. Another melting endotherm is visible at 15 °C in the total heat flow, just before the endotherm of the evaporation of water. It is worth noticing that the polymers from which the EG/VA consists of have similar melting temperatures. PEG 600 (Mw = approx. 600 g/mol) has a melting temperature of ca. 20–25 °C, and PVA 9500 (Mw = approx. 9500 g/mol) has a melting temperature of ca. 180°. Two exothermic signals are visible in the cooling curve (Fig. 1B), due to the crystallization of the two phases. The first one, at around 180 °C, is the crystallization of the phase that melts at 212 °C. The second exothermic peak at −35 °C was the crystallization of the phase that melts at 15 °C (Fig. 1B).

A first glass transition at −57 °C (ΔCp = ca. 0.14 J/g °C, Fig. 1C) and a second one around 45 °C (ΔCp = ca. 0.21 J/g °C, Fig. 1A) can be noticed in the reversing heat flow. The second glass transition is difficult to determine because of the rather broad endothermic melting signal before it. Therefore, a program that heated the sample till 40 °C (so melting could occur) and then cooled it till −15 °C was applied, so crystallization did not occur in these conditions. Reheating till 100 °C showed no endothermic melting signal, and the glass transition was now clearly visible and could be determined to be at 50 °C (Fig. 1D). This is slightly higher than it was before, probably due to different thermal history and the ability to set the limits more accurately.

The MDSC results obtained clearly indicate that PEG forms a separate fraction. This fraction has a glass transition temperature at −57 °C and a melting endotherm at 15 °C and will be further referred to as 'PEG fraction'. There is also a second fraction with a glass transition temperature around 45 °C (or 50 °C after heat–cool–heat) and a melting endotherm at 212 °C, this fraction is further indicated as 'PVA fraction'.

3.1.2. XRPD results

The pure unprocessed EG/VA was analyzed at room temperature with XRPD using the Bragg–Brentano technique with the flat sample holders (Fig. 2). The most intense peak occurs at 19.5° and has a shoulder peak at 22.6°. The next intense peak is visible

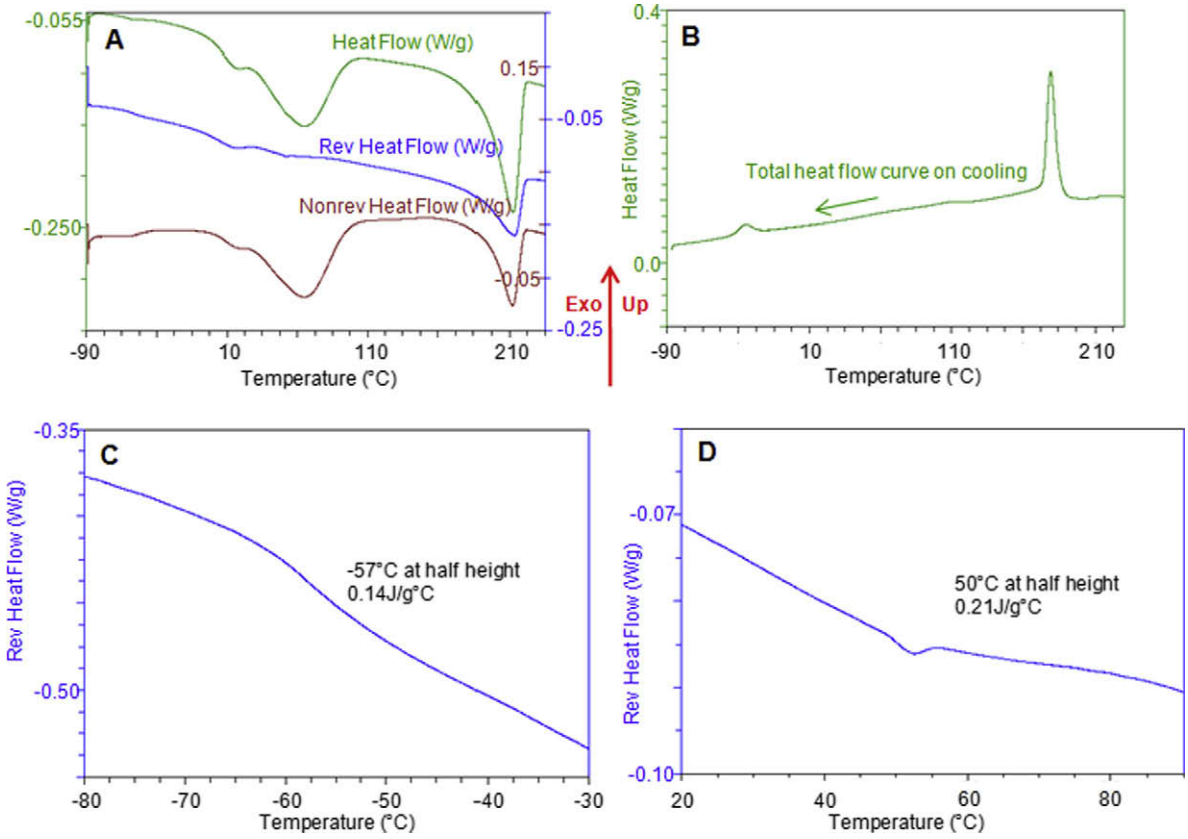

Fig. 1. MDSC of unprocessed poly(ethyleneglycol-g-vinylalcohol). (A) The total, reversing and non-reversing heat flow. (B) The total heat flow curve on cooling. (C) A close-up of the first glass transition at −57 °C. (D) A close-up of the second glass transition after cooling till −15 °C.

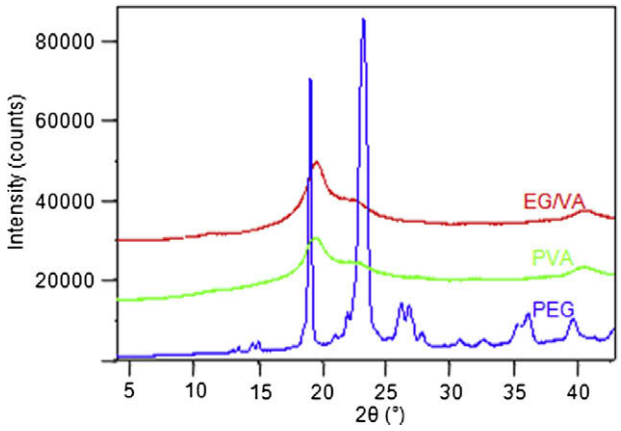

Fig. 2. XRPD of pure EG/VA, PVA and PEG using the Bragg–Brentano geometry with the flat sample holder.

at 40.5°, and another small peak is visible at 11.3°. Polyvinylalcohol (PVA, Mw = 9500) and polyethyleneglycol (PEG, Mw = 2000) were also analyzed. PVA showed a similar pattern; the peaks are positioned at the same angles, the largest peak again at 19.5°, concurring with data reported by Ali et al. [12] and a shoulder peak at 22.6°. PEG showed two peaks at 19.1° and 23.2°, according to the data of Corrigan et al. [13]. Peaks of PEG are not present in the diffractogram of EG/VA, due to the fact that the PEG fraction is in the molten state, having a melting temperature of 15 °C, hence confirming the MDSC data.

3.2. Influence of the spray-drying process/formulation parameters on the pure EG/VA

3.2.1. The inlet temperature

EG/VA was spray dried from a 5% (w/v) solution in water using different inlet temperature settings (Table 1). The MDSC results show no change in the ΔCp of the first glass transition at −57 °C and a slight increase in ΔCp of the second glass transition with decreasing inlet temperature (Fig. 3). The ΔCp of T_{g2} of the spray-dried product after spray-drying at 170 °C is smaller than the ΔCp of the pure EG/VA. The diffractogram of the product spray dried using an inlet temperature of 170 °C has a sharper peak at 19.5° and a more pronounced (sharper) shoulder at 22.5° (Fig. 4). The peak intensity and sharpness are clearly decreasing with decreasing inlet temperature.

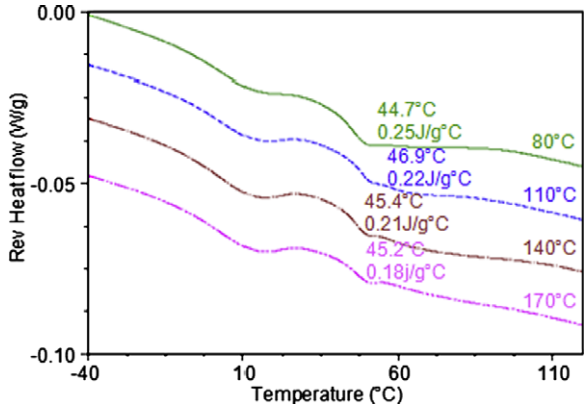

Fig. 3. Overlay of reversing heat flow curves of spray-dried EG/VA at different inlet temperatures. All the products were spray dried from a 5% (w/v) solution of EG/VA in water. The different inlet temperatures are indicated in the figure (80°, 110°, 140°, 170 °C). The ΔCp of the second T_g is indicated in each thermogram, the ΔCp of unprocessed EG/VA was ca. 0.21 J/g °C.

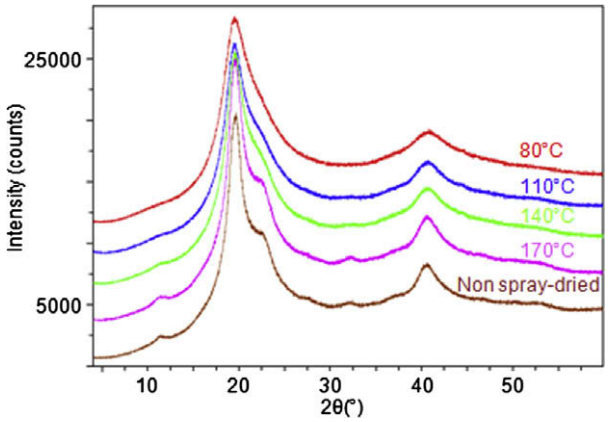

Fig. 4. XRPD of the spray-dried EG/VA using the Bragg–Brentano geometry with the flat sample holder. The different spray-drying inlet temperatures are indicated in the figure (80, 110, 140, 170 °C). The diffractogram of the unprocessed EG/VA is also displayed as a reference.

The MDSC and XRPD results of the products spray dried with different inlet temperatures point out that the amorphous part of the PEG fraction is not influenced by the spray-drying process, but that the amorphous part of the PVA fraction of the copolymer has a higher amorphous content after spray-drying at temperatures lower than 170 °C.

3.2.2. The solvent

Three different solvents or mixtures were tested, 100% H_2O, 50% H_2O–50% EtOH and 25% H_2O–50% EtOH–25% CH_2Cl_2. EG/VA was always first dissolved in water, before adding any other solvent. All three spray-dried products had a higher amorphous content than the pure EG/VA, because the peak at 19.5° and the shoulder at 22.6° are less sharp (Fig. 5). MDSC results showed no significant change in ΔCp of the first or the second glass transition between the three spray-dried products (data not shown).

The results obtained indicate that the solvents used have little or no influence on the crystallinity of the spray-dried polymer.

3.2.3. Influence of plasticizers

Glass transition temperatures of the spray-dried EG/VA with and without plasticizer at different concentrations are given in Table 3. PEG400, propyleneglycol and diethyl phthalate were added to the spray-drying solution as plasticizers in 10% or 30%

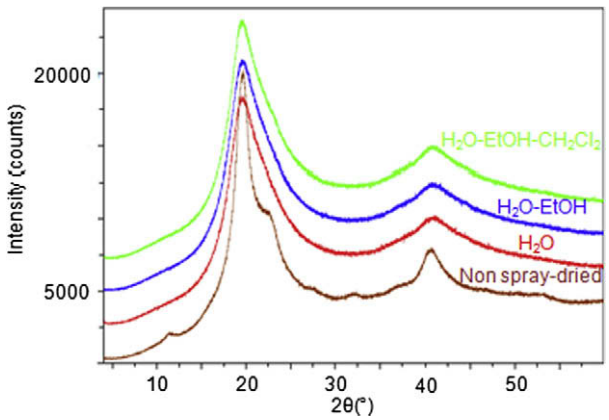

Fig. 5. XRPD of spray-dried EG/VA using the Bragg–Brentano geometry with the flat sample holder. The solvent mixtures used for preparing the spray-drying solutions are indicated in the figure (H_2O, H_2O–EtOH, H_2O–EtOH–CH_2Cl_2). The inlet temperature was kept constant at 80 °C.

Table 3
Overview of the glass transition temperatures of different spray-dried products with and without plasticizer.

	T_{g1} (°C)	T_{g2} (°C)
5% EG/VA in H_2O, inlet *T* 110 °C	−57.3	45.9
5% EG/VA in 1:1 H_2O–EtOH, inlet *T* 90 °C	−58.0	47.0
10% Plasticizer		
Propyleneglycol	−58.0	46.6
PEG400	−59.5	43.0
Diethyl phthalate	−62.9	46.9
30% Plasticizer		
Propyleneglycol	−56.5	46.0
PEG400	−63.3	35.7
Diethyl phthalate	−69.0	47.2

(w/w%) relative to the amount of EG/VA added to the solution. Water was used as a solvent for the solutions of propyleneglycol and PEG400, and the inlet temperature was set to 110 °C. A mixture of water and ethanol (1:1) was used for the solutions with diethyl phthalate, with the inlet temperature set at 90 °C. In the reference solution of 5% EG/VA in 100 ml H_2O with an inlet temperature of 110 °C, the glass transitions were determined to be at −57.3 °C and 45.9 °C, in the solution of 5% EG/VA in 100 ml 1:1 H_2O–EtOH mixture, the glass transitions were determined to be at −58.0 °C and 47.0 °C.

The glass transition temperatures of the spray-dried products with propyleneglycol did not show any change. 10% PEG400 made the second glass transition shift to 43.0 °C, and 30% PEG400 made both glass transitions shift; the first one to −63.3 °C, but the second one was difficult to determine accurately, because of the presence of a melting endotherm of PEG400 interfering within the region of the second glass transition. Therefore, a program that heated the sample till 40 °C (so melting could occur) and then cooled it till −15 °C was applied, so crystallization did not occur in these conditions. Reheating till 100 °C showed no endothermic melting signal in the glass transition region, the glass transition temperature could now be determined to be at 35.7 °C. Diethyl phthalate had an influence on the first glass transition. Addition of 10% of diethyl phthalate made the first glass transition shift to −62.9 °C, while addition of 30% of diethyl phthalate in the polymer made it shift to even −69.0 °C; the second glass transition remained constant.

Depending on the type of plasticizer and the concentration of the plasticizers, different results were obtained. Certain plasticizers have preference for certain amorphous phases in the EG/VA. Also, the amount of plasticizer can give different results. Diethyl phthalate has a preference for the amorphous phase of the PEG fraction, in each tested concentration, while PEG400 in lower concentration (10% w/w) has a preference for the amorphous phase of the PVA fraction, but at higher concentration (30% w/w) it can also influence the amorphous phase of the PEG fraction. Theoretically, it can be expected that drug molecules which are also small organic molecules act similarly. Depending on the type and concentration of the drug, different mixing behavior can occur.

3.3. Influence of hot-melt extrusion process parameters on the pure EG/VA

3.3.1. The extrusion temperature

While keeping the rotation speed and circulation time constant (44 rpm and 5 min), the processing temperature was varied in the co-rotating twin screw extruder. Previously, Janssens et al. [6] used an extrusion temperature of 180 °C for extruding EG/VA–itraconazole blends. The temperature was chosen to make sure all the itraconazole in the mixture was molten. Since EG/VA already starts to decompose at 170 °C, it is more interesting to extrude at lower

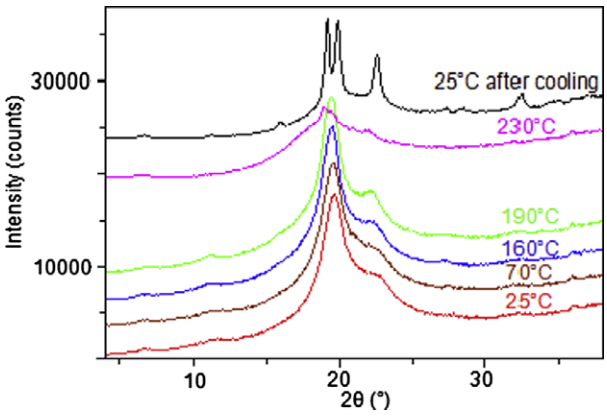

Fig. 6. Diffractograms of EG/VA at different temperatures (Anton Paar non-ambient chamber). The unprocessed EG/VA was first cooled down till −90 °C and then heated till 230 °C in different steps, the diffractogram at 25°, 70°, 160°,190° and 230 °C are shown. Subsequently, the material was cooled again to 25 °C (upper curve).

temperatures. In our experimental set-up, temperature was varied from 180 °C to 130 °C as indicated in Table 2. As the temperature was lowered, the extrudates were more transparent and less colored brown/yellow due to less decomposition. A temperature of 130 °C was too low to extrude the copolymer; the material remained as powder.

MDSC showed no change in ΔCp of the first T_g (ΔCp = ca. 0.14 J/g °C), the second T_g is no longer visible after extrusion, strongly suggesting that the amorphous phase of the PVA part becomes more crystalline. It is remarkable that the enthalpy of fusion of the second melting endotherm remained constant when comparing extruded and non-extruded samples (ΔHf_2 = ca. 62 J/g), most likely pointing to cold crystallization occurring during the MDSC measurement. XRPD spectra recorded at different temperatures are shown in Fig. 6. When the material is heated to 70, 160 and 190 °C, the diffraction peak at 22.6° becomes sharper, confirming the cold crystallization at elevated temperatures. At 230 °C, the peaks flatten again, because of the material that has melted. The double peak at 19.2° and 19.9° and the intense peak at 22.6° were also visible in the diffractogram of EG/VA that was simply heated to 230 °C and then cooled (Fig. 6, top diffractogram).

Fig. 7 shows the diffractograms of the different extruded samples, measured using the transmission geometry. The temperature of extrusion is indicated in the figure. The diffractograms of unprocessed EG/VA and unprocessed PVA and PEG are shown as reference. The XRPD spectra of the extruded EG/VA show more intense diffraction peaks than the unprocessed EG/VA, indicating that the crystallinity increases after extrusion. The extruded samples display two major peaks at 19.2° and 20.0° and three other minor peaks at 11.2°, 16.0° and 22.7°. The shoulder peak of unprocessed EG/VA at 22.7° has increased in intensity, and the broad peak at 19.5° is split up in two separate sharp peaks. Also, the small peak at 11.2° became more intense after extrusion. Unprocessed PEG shows two major peaks, one at 19.1° and one at 23.3°, hence no peak corresponds to those of EG/VA. The most intense peak of PVA is at 19.5° and a shoulder peak at 22.7°; this shoulder peak corresponds to the peak at 22.7° of the (extruded) EG/VA. After extrusion of PVA, its diffraction pattern also changes as shown in Fig. 8. Instead of the broad peak at 19.5°, two peaks occur at 19.2° and 19.9°. Also, the peak at 22.7° increases in intensity. The double peak of extruded PVA corresponds to the double peak of extruded EG/VA (in both cases, extrusion parameters were set at 160 °C, internal circulation time of 5 min, rotation speed of 44 rpm and an internal circulation time of 5 min). These results prove that EG/VA becomes more crystalline after extrusion. The

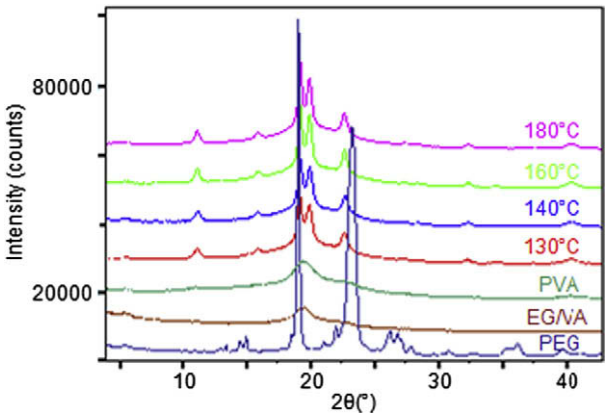

Fig. 7. XRPD of the extrudated samples using the transmission geometry. The extrusion temperature was varied, while keeping screw speed and circulation time constant (44 rpm and 5 min). The temperatures are indicated in the different diffractograms (130°, 140°, 160°, 180 °C). The XRPD of the unprocessed EG/VA and the unprocessed PVA and PEG measured with the same geometry are also displayed as reference.

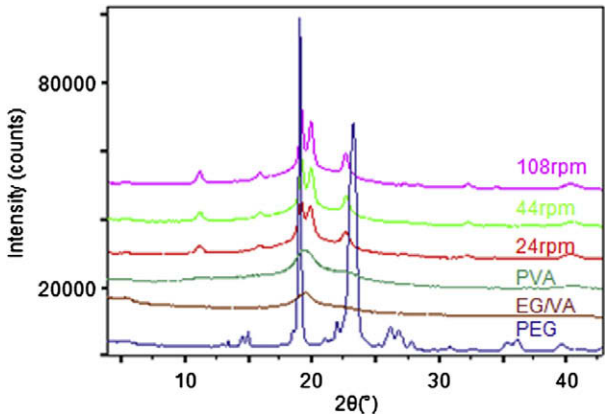

Fig. 9. XRPD of the extrudated samples using the transmission geometry. The screw speed was varied, while keeping the extrusion temperature and circulation time constant (140 °C and 5 min). The different screw speeds are indicated on the diffractograms (24, 44, 108 rpm). The XRPD of the unprocessed copolymer EG/VA and the unprocessed polymers PVA and PEG measured using the same geometry are also displayed as reference.

crystallinity of the PEG fraction remains the same, while crystallinity of the PVA fraction of EG/VA clearly increases.

3.3.2. The rotation speed

As already shown in Fig. 6, the heat applied to the material during the hot-melt extrusion process clearly has an influence on the phase behavior of EG/VA. Since hot-melt extrusion is a combination of heat and shear forces that are exerted on the extruded material, a next set of experiments was conducted in order to estimate the contribution of shear forces on the increase of EG/VA crystallinity.

The influence of shear forces was studied by varying the screw rotation speed at 24 rpm, 44 rpm and 108 rpm (Table 2), and the temperature and circulation time were kept constant (140 °C and 5 min). This temperature was chosen, because it was the lowest temperature that allowed making acceptable extrudates.

MDSC showed no change in ΔCp of the first T_g (ΔCp = ca. 0.14 J/g °C), the second T_g is still visible in the thermogram of the extruded sample with rotation speed 24 rpm, but no longer when the rotation speed was set at 44 rpm or 108 rpm. These results are confirmed in the diffractograms of the extruded EG/VA in Fig. 9. The double peak at 19.2° and 20.0° and the smaller peaks at 11.2°, 16.0° and 22.7° increase in intensity with increasing rotation speed indicating that increased crystallinity of the material after extrusion is also due to the presence of shear forces in the extruder. Nevertheless, the enthalpy of fusion of the second melting peak remains again the same (ΔHf_2 = ca. 62 J/g) for the processed and unprocessed EG/VA, again strongly suggesting that cold crystallization probably occurs during the MDSC measurement.

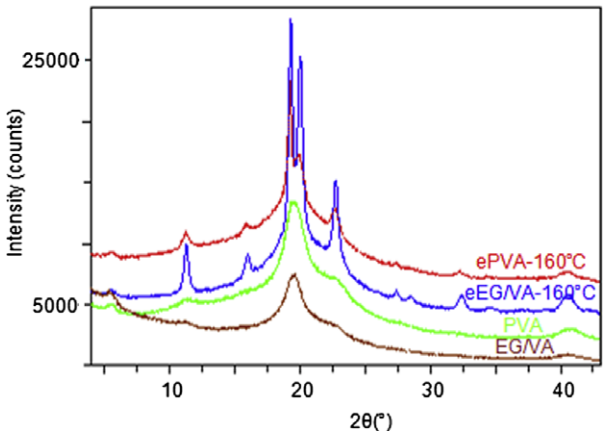

Fig. 8. XRPD of (extruded) EG/VA and PVA using the transmission geometry. The extrusion temperature was set to 160 °C with a rotation speed of 44 rpm and circulation time of 5 min.

3.4. Influence of cooling rate on EG/VA

Although cooling at ambient temperature is generally performed of extrudates, it is possible to adapt extruders, so that forced cooling of the extrudates takes place. The extrudates can be pushed through a die that is kept at low temperatures to apply a forced cooling. During processing, polymers can be subject to cooling rates in excess of 1000 °C/min [14,15]. Therefore, we investigated the possibility to make the polymer amorphous by quench cooling. EG/VA was therefore wrapped in aluminum foil and cooled to −120 °C, followed by heating it to 250 °C at 100 °C/min and kept isothermal there for one minute in order to allow melting of the sample. Next, the sample was cooled at different rates; 100, 200, 300, 400 and 500 °C/min, all by using HPer DSC. This technique allows heating and cooling rates up to 500 °C/min over a broad temperature range [15]. The cooling curves are shown in Fig. 10. The exothermic signals are the crystallization transitions of the PVA part of EG/VA. These crystallization peaks shift to lower temperatures if cooling rate increases. When cooling at 100 °C/min, crystallization occurs at approximately 173 °C, while it drops to approximately 141 °C when a cooling rate of 500 °C/min is applied, all values being corrected for the scan rates used. These high cooling rates were not sufficient to make the EG/VA amorphous, therefore ultra-fast chip calorimetry was used since much higher cooling rates can then be reached.

The samples were heated from −180 °C to 260 °C using a heating rate of 10,000 °C/s, subsequently, they were cooled at different cooling rates varying from 100 °C/s to 20,000 °C/s. The first part of the cooling (till 187 °C) was always performed at 10,000 K/s, to make sure that the degradation of the product at these high temperatures was kept to a minimum. After cooling at these different rates, the samples were reheated at 10,000 °C/s. These second heating curves are displayed in Fig. 11. It was not possible to obtain reliable data in the whole range of cooling rates applied, because the sample mass was too low to have a good signal at the slowest cooling rates. The melting peak is situated at ca. 190 °C, where it

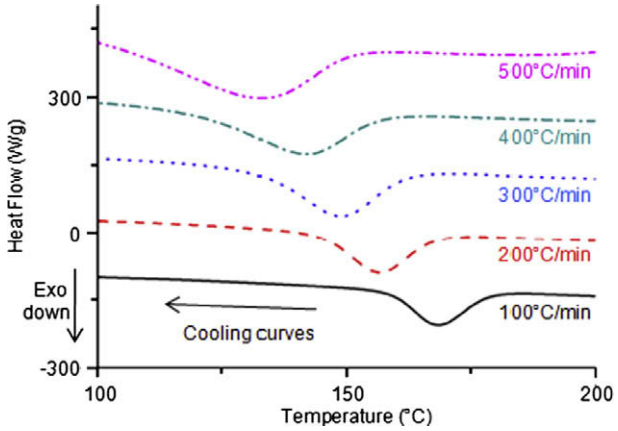

Fig. 10. Overlay of the HPer DSC results of unprocessed EG/VA, the curves are the cooling curves after heating at 100 °C/min. The different cooling rates are displayed in the figure.

lies normally around 210 °C. The reduction of melting temperature could be due to reduced reorganization on heating as it is commonly observed on slow heating rates (DSC) [16].

The two glass transitions are clearly visible and indicated with solid arrows in Fig. 11, the first one at ca. −60 °C and the second one at ca. 80 °C. Why the first glass transition temperature is lower than in the MDSC scans is not yet known and may indicate some uncertainty in the temperature measurements or could be due to the fully amorphous state of the PEG fraction, see below. The second glass transition is higher compared to the MDSC measurements as it is expected because of the much higher heating rate. The first glass transition does not change in ΔCp with increasing cooling rate, and the first melting endotherm that is visible in our previous MDSC curves is not visible in these curves, indicating that this fraction is completely amorphous. The heating curves after cooling at 300, 500 and 800 °C/s show no cold crystallization,

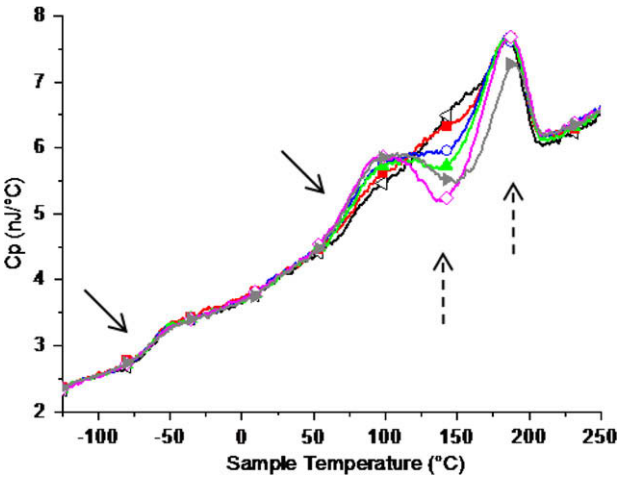

Fig. 11. Overlay of the ultra-fast chip calorimetry thermograms. The sample of EG/VA was cooled at different cooling rates and subsequently heated at 10,000 °C/s. These heating curves are shown here. The black curve with the open left triangle is the heating curve after cooling at 300 °C/s, the red curve with the solid square is the heating curve after cooling at 500 °C/s, the blue curve with the open dot is the heating curve after cooling at 800 °C/s, the green curve with the solid up triangle is the heating curve after cooling at 1000 °C/s, the pink curve with the open diamonds is the heating curve after cooling at 3000 °C/s and the grey curve with the solid right triangle is the heating curve after cooling at 20,000 °C/s. The solid arrows indicate the two glass transitions, and the dashed arrows indicate the cold crystallization and melting of the copolymer. (For interpretation of the references to color in this figure legend, the reader is referred to the web version of this article.)

only melting (both transitions indicated with the dashed arrows in Fig. 11). The second glass transition becomes more pronounced with increasing cooling rate indicating the increase of the amorphous fraction of the PVA part with increasing cooling rate. Cold crystallization could be observed before the EG/VA melts (indicated with the dashed arrows in Fig. 11) in the second heating curve after cooling at 1000 °C/s or higher. The cold crystallization becomes more pronounced with increasing cooling rates, while the ΔCp of the second glass transition remains the same. The area under the curve of the cold crystallization and the melting are comparable when a cooling rate of 3000 K/s or higher is applied. This indicates that the PVA fraction becomes completely amorphous, since only the crystals formed during cold crystallization melt.

The cold crystallization decreases again after cooling at 20,000 °C/s, due to an increasingly reduced number of nuclei formed at increasing cooling rates[17].

4. Conclusion

In this paper, we described the phase behavior of pure EG/VA before, during and after typical solid dispersion manufacturing processes like spray-drying and hot-melt extrusion. EG/VA as received from the manufacturer consists of two semi-crystalline fractions. One fraction (the 'PEG fraction') has a glass transition (T_g = −57 °C) and melting endotherm (T_m = 15 °C) similar to PEG, while the other one (the PVA fraction) has a glass transition (T_g = 45 °C) and melting endotherm (T_m = 212 °C) that is similar to PVA, indicating that the PEG part does not act as an internal plasticizer as suggested by the manufacturer, but as a separate moiety. Both parts are semi-crystalline, and both phases can be influenced differently by solid dispersion manufacturing methods such as spray-drying and hot-melt extrusion.

Mixtures of organic solvents allow spray-drying of EG/VA out of a single solution. The spray-dried EG/VA is more amorphous (mainly the PVA fraction) than the starting material if the inlet temperature is kept below 170 °C, allowing small organic molecules (like drug molecules) to be more easily dispersed in one or two of the amorphous phases. Tests with 3 different plasticizers indicated that depending on the type and the concentration of the compound, a different preference for one of the two amorphous phases can occur. This suggests that also small organic compounds like drugs may preferentially mix with one of the two amorphous phases of EG/VA during solid dispersion manufacturing. This can lead to different physical stability profiles, depending on which amorphous phase is involved in mixing.

Acceptable extrudates of EG/VA were obtained with hot-melt extrusion when applying a processing temperature of 140 °C, a screw speed of 44 rpm, an internal circulation time of 5 min and a load of 5 g. At elevated temperature, oxidation takes place, and EG/VA becomes yellow/brown colored. Hot-melt extrusion increases the crystallinity of the PVA fraction of the material as a consequence of the effect of both temperature and shear forces. The PEG fraction is not affected. When the addition of a small organic drug compound can plasticize the material an even lower process temperature will result. The combination of a relatively low process temperature and the remaining amorphous character points to be the potential of this material as a carrier for solid dispersions manufactured by hot-melt extrusion.

Controlled quench cooling rates up to 500 °C/min obtained by HPer DSC could delay but not avoid crystallization. Ultra-fast chip calorimetry experiments showed that a cooling rate of 3000 °C/s was necessary to make to EG/VA completely amorphous, indicating that applying forced cooling after extrusion in order to make the extrudates completely amorphous is almost impossible.

Acknowledgements

SG and PK acknowledge the Institute for the Promotion of Innovation through Science and Technology in Flanders (IWT-Vlaanderen) for a Ph.D. Grant.

The authors acknowledge the financial support from K.U.L. Industrial Research Fund (IOF-KP/06/021) and FWO-Vlaanderen (G.0614.07).

The support of TP and VM by PerkinElmer Shelton, CT, USA is appreciated.

References

[1] C. Lipinski, Poor aqueous solubility – an industry wide problem in drug discovery, Am. Pharm. Rev. 5 (2002) 82–85.
[2] W.L. Chiou, S. Riegelman, Pharmaceutical applications of solid dispersion systems, J. Pharm. Sci. 60 (1971) 1281–1302.
[3] T. Vasconcelos, B. Sarmento, P. Costa, Solid dispersions as strategy to improve oral bioavailability of poor water soluble drugs, Drug Discovery Today 12 (2007) 1068–1075.
[4] BASF Aktiengesellschaft, Technical Information, Kollicoat IR®, 2001.
[5] K. Kolter, M. Gotsche, T. Schneider, Physicochemical characterization of Kollicoat IR®, BASF ExAct 8 (2002) 2–3.
[6] S. Janssens, H. Novoa de Armas, J.P. Remon, G. Van den Mooter, The use of a new hydrophilic polymer, Kollicoat IR®, in the formulation of solid dispersions of itraconazole, Eur. J. Pharm. Sci. 30 (2007) 288–294.
[7] S. Janssens, M. Anné, P. Rombaut, G. Van den Mooter, Spray drying from complex solvent systems broadens the applicability of Kollicoat IR as a carrier in the formulation of solid dispersions, Eur. J. Pharm. Sci. 37 (2009) 241–248.
[8] T.F.J. Pijpers, V.B.F. Mathot, B. Goderis, R.L. Scherrenberg, E.W. van der Vegte, High-speed calorimetry for the study of the kinetics of (de)vitrification, crystallization, and melting of macromolecules, Macromolecules 35 (2002) 3601–3613.
[9] S.A. Adamovsky, A.A. Minakov, C. Schick, Scanning microcalorimetry at high cooling rate, Thermochim. Acta 403 (2003) 55–63.
[10] A.A. Minakov, C. Schick, Ultrafast thermal processing and nanocalorimetry at heating and cooling rates up to 1 MK/s, Rev. Sci. Instrum. 78 (2007) 073902.
[11] Y.L. Gao, E. Zhuravlev, C.D. Zou, B. Yang, Q.J. Zhai, C. Schick, Calorimetric measurements of undercooling in single micron sized SnAgCu particles in a wide range of cooling rates, Thermochim. Acta 482 (2009) 1–7.
[12] Z.I. Ali, F.A. Ali, A.M. Hosam, Effect of electron beam irradiation on the structural properties of PVA//V_2O_5 xerogel, Spectrochim. Acta Part A 72 (2008) 868–875.
[13] D.O. Corrigan, A.M. Healy, O.I. Corrigan, The effect of spray drying solutions of polyethylene glycol (PEG) and lactose/PEG on their physicochemical properties, Int. J. Pharm. 235 (2002) 193–205.
[14] R.L. Danley, P.A. Caulfield, S.R. Aubuchon, A rapid-scanning differential scanning calorimeter, Am. Lab. (January) (2008) 9–11.
[15] V.B.F. Mathot, G. Vanden Poel, T.F.J. Pijpers, Benefits and potentials of high performance differential scanning calorimetry (HPer DSC), in: M. Brown, P. Gallagher (Eds.), Handbook of Thermal Analysis and Calorimetry, Recent Advances Techniques and Applications, vol. 5, Elsevier, Amsterdam, 2007, pp. 269–297.
[16] A.A. Minakov, D.A. Mordvintsev, C. Schick, Melting and reorganization of poly(ethylene terephthalate) on fast heating (1000 K/s), Polymer 45 (2004) 3755–3763.
[17] M. Salmerón Sánchez, V.B.F. Mathot, G. Vanden Poel, J.L.G. Ribelles, Effect of the cooling rate on the nucleation kinetics of poly(L-lactic acid) and its influence on morphology, Macromolecules 40 (2007) 7989–7997.